

**A Contact Angle Study of Processing Induced Changes to
InGaZnO₄ and Lotus Glass surface**

A Thesis
Presented to the Faculty of the Graduate School
of Cornell University
In Partial Fulfillment of the Requirements for the Degree of Master of Science

by
Wenjin Zhang
January 2016

© 2016 Wenjin Zhang

ABSTRACT

The carrier density in amorphous indium gallium zinc oxide (a-IGZO) thin film transistors is critical for optimal device operation. While doping is known to be controlled by processing steps such as thermal anneals, little focus has been given to the effect of other fabrication process steps, such as photolithography, on carrier concentrations. Thin-film device characteristics are, however, known to depend on these low temperature processes.

The role of one specific lift off photographic process (LOR) to IGZO thin film has been examined in this work. Results show that this LOR process modifies the IGZO surface and that the effect occurs almost instantly and is permanent. We propose that hydrogen doping into the IGZO layer from acids in the photoresist increases the carrier concentration of the films.

The effect of hydrogen plasma treatment on commercial TFT glass substrates was also explored. The contact angle of the glass surface after hydrogen plasma treatment was investigated to follow the surface energy changes. The results show the surface becoming hydrophobic after hydrogen plasma treatment, with the surface gradually returning to a hydrophilic condition. These data also suggest hydrogen diffusion into glass surface during the plasma treatment.

BIOGRAPHICAL SKETCH

Wenjin Zhang is from Anhui, China and received her bachelor's degree from Tsinghua University in 2013. She majored in Chemistry and completed two projects during her undergraduate studies. The first project focused on improving the performance of OTFT devices under three different ISQ compositions and the second involved synthesizing Cu(I) nanoparticles as catalyst, for C-N coupling reactions. Upon completing her bachelor's degree, she came to Cornell University and joined Prof. Michael Thompson's group to pursue Master of Science degree in September 2013. At Cornell, she completed a project on the role of processing on IGZO and Lotus Glass using contact angle techniques.

ACKNOWLEDGEMENTS

I want to express my appreciation to my parents and my twin sister. They supported me with unconditional love and are always at my back when I met problems.

I would like to thank my advisor Prof. Michael Thompson for his full support and expert guidance. He is always very patient and gave me lots of suggestions and encouragement for my study and research. This dissertation would not have been possible without his kind help. I would also like to thank Prof. Dieter Ast for sharing his great experience and encyclopedic knowledge with us. He gave us his advice without reservation and I learned a lot from him.

It's my great pleasure to work with my subgroup teammates Bin Zhu, David Lynch, Chenyang Chung and Kathryn Roach. Bin has a strong background of glass and he provided me with a lot of useful suggestions when I met some result I couldn't explain. David is so nice that I can always get help from him whenever I have problems. Chenyang has been in our group for longest time. He is a great friend of mine, and has helped me with my research as well as course study. Kate also gave me a lot of useful advise and was willing to share her experimental experience.

I would also like to thank all my friends who have accompanied me for the great two years in Cornell. They supported me with great help and encouraged me during my difficult times. They made my study life extremely meaningful.

I would like to thank Raymond Greene, Corning Inc. and staff at the Cornell NanoScale Facility. For all people mentioned above, you are the reason this dissertation could happen and I'm so grateful to have you all in my life.

TABLE OF CONTENTS

1. Introduction	1
2. Experimental Details	6
2.1 Thin Film Deposition by Sputter	6
2.2 Photolithography Process	11
2.3 PECVD	14
2.4 Characterization	16
2.4.1 Contact Angle	16
2.4.2 4-Point Probe Measurement.....	18
2.4.3 Atomic Force Microscope	19
3. Results and Discussions.....	20
3.1 IGZO Film Surface	20
3.1.1 Storage Conditions.....	20
3.1.2 Surface Changes with Time.....	22
3.1.3 Effect of LOR Treatment to IGZO Thin Film Conductivity.....	23
3.1.4 LOR Post-baking Temperature.....	24

3.1.5 Film Conductivity after Annealing	28
3.1.6 Discussion.....	31
3.2 Glass Surface	33
3.2.1 PECVD Treated Glass Surface.....	33
3.2.2 Surface Roughness	36
4. Conclusions	38
References	40

LIST OF FIGURES

Figure 1 Top gate and bottom gate oxide TFTs structures by Jin-Seong Park [10]	2
Figure 2 Sputter deposition system	7
Figure 3 Schematic diagram of three modes of film growth	9
Figure 4 Typical wafer anneal furnace.....	10
Figure 5 Steps of a photolithography process	12
Figure 6 Steps of lift off process.....	13
Figure 7 Structure of PECVD	15
Figure 8 Contact angle of (a) a hydrophobic surface and (b) a hydrophilic surface..	16
Figure 9 Definition of the contact angle formed by liquid drop and solid surface	17
Figure 10 4-point probe	18
Figure 11 Contact angle changes with storage time for uncoated IGZO sample and LOR 5A coated IGZO sample	22
Figure 12 Contact angles of IGZO samples after LOR treatment at different temperatures.....	25
Figure 13 Current sweep for IGZO samples after LOR treatment.....	26

Figure 14 Carrier concentration of IGZO film after LOR treatment	27
Figure 15 (a) Contact angle (b) current sweep curve for 350°C annealed IGZO sample	28
Figure 16 Current sweep curve of IGZO sample for (a) annealed with N ₂ at 205°C for 5 min (b) LOR treatment with 205 °C baking for 5 min	29
Figure 17 Contact angle of IGZO samples annealed in N ₂ at 350°C followed by post anneal with LOR at different temperatures	30
Figure 18 Carrier density as a function of the inverse LOR bake temperature.....	32
Figure 19 Contact angle of glass (a) before oxygen plasma (b) after an oxygen plasma clean	33
Figure 20 Contact angle changes with time after hydrogen plasma	35
Figure 21 Surface roughness of glass surface	36

LIST OF TABLES

Table 1 Molecule diffusion in fused silica glass from Narottam P. Bansal	4
Table 2 Contact angle of IGZO samples under different storage conditions	21
Table 3 Sheet resistance for IGZO film before and after LOR treatment.....	24
Table 4 Effect of LOR bake temperatures on IGZO properties	27
Table 5 Estimated carrier concentration for samples treated with LOR 5A after a 350 ⁰ C furnace N ₂ anneal.....	31
Table 6 Contact angle of glass surface after hydrogen plasma treatment.....	34

1. Introduction

IGZO, which refers to indium gallium zinc oxide, is a revolutionary transparent compound semiconductor first reported by Hosono in 2004 [1]. As a member of the amorphous oxide semiconductors, IGZO is seen to be a potential replacement for amorphous silicon [2]. Although amorphous silicon has dominated the flat-panel display market, it has a relative low mobility ($<1 \text{ cm}^2/\text{Vs}$) and exhibits an instability under electric stress. IGZO has been shown to be competitive in flexible thin film transistors (TFTs) with improved device performance. Compared with TFTs fabricated with a-Si, IGZO TFTs have mobilities near $10 \text{ cm}^2/\text{Vs}$ and can be deposited at room temperature [3]. Uniform thin films are easy to obtain using sputter deposition and can be generated with high carrier concentrations for applications [4].

The fabrication process of IGZO TFT device has been widely investigated to improve the device performance [5]. Deposition can be optimized by controlling the oxygen partial pressure and rf power during sputter [6], or cosputtering of IGZO and IZO (indium zinc oxide) to reduce the interface trap density [7]. Post annealing treatment of devices, either by furnace anneal [8] or laser anneal [9], significantly improves not only the mobility but also the stability and uniformity of TFTs.

There are two common used geometries for oxide TFT device, a top gate structure and a bottom gate structure (Figure 1). The function of the semiconductor is to modulate current flow through the channel layer from the source and drain

electrodes, with conductivity induced by an vertical electric field created in the semiconductor by the gate charge between the gate and drain [10].

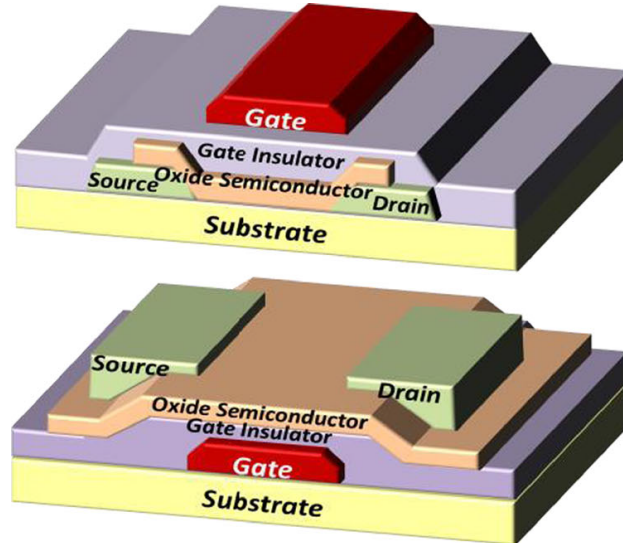


Figure 1 Top gate and bottom gate oxide TFTs structures by Jin-Seong Park [10]

Traditional semiconductor processing is used to fabricate these TFTs. One of these processes is a lift-off used to pattern multiple layer deposition. A specific lift off resist (LOR) is used to protect the unexposed area during deposition [11]. We normally expect this lift off resist process to be extremely clean and to have no effect on the IGZO surface or further process steps. However, during TFT fabrication we occasionally observed that the LOR process significantly affected IGZO device characteristics. IGZO appears to be very sensitive to the processing environment and especially to LOR in direct contact with IGZO during lift off processes. How LOR processing actually affects the IGZO surface is not known. In this work, we attempt to gain a fundamental understanding of how this photolithograph process modifies

the IGZO layer, with a goal of ultimately gaining better control of the process and the properties of devices.

Contact angle is a sensitive parameter of surface structure, which can be used to monitor surface energy changes. The contact angle is extremely sensitive and very small modifications can be readily detected by the measurement. Four point probe electrical measurements were also used in my experiments to estimate the sheet resistance and carrier concentration of IGZO thin film. Our results demonstrate the effect of LOR process on IGZO is nearly instantaneous and permanent, and we suggest hydrogen doping into the IGZO layer is the underlying mechanism for the increase in carrier concentration.

Glass is almost universally the substrate for transparent flexible TFT device fabrication [12]. Knowledge and control of the glass surface is critical in order to fabricate functional devices on these substrates. Deposited materials must adhere to the surface to achieve a flat and uniform film. The interaction between deposited films and the substrate is also critical for the stability of devices.

Hydrogen plasma can be used to clean glass surfaces prior to other fabrication steps in industrial processes [13]. Surface wrinkling under hydrogen plasma has been occasionally observed, which motivates our interests in understanding the surface behavior under hydrogen plasma. In this work, we examined the effect of hydrogen plasma on glass substrate in order to understand the role of process environments.

Table 1 Molecule diffusion in fused silica glass from Narottam P. Bansal [14]

Molecule	Diameter (Å)	Diffusion coefficient (cm ² s ⁻¹)		Activation energy Q' (kJ mole ⁻¹)
		25°C	1000°C	
Helium	2.0	2.4×10^{-8}	5.5×10^{-5}	20
Neon	2.4	5×10^{-12}	2.5×10^{-6}	37
Hydrogen (deuterium)	2.5	2.2×10^{-11}	7.3×10^{-6}	36
Argon	3.2		1.4×10^{-9}	111
Oxygen	3.2		6.6×10^{-9}	105
Water	3.3		$\sim 3 \times 10^{-7}$	71
Nitrogen	3.4			110
Krypton	4.2			~ 190
Xenon	4.9			~ 300

The diffusivity of hydrogen in glass is relative low even under high temperature (Table 1) [14]. This effect was confirmed by J. B. Brady [15]. The presence of Eu³⁺ and Al³⁺ in glass can increase the solubility of hydrogen, which indicates that substrate structure modifications have a significant effect on hydrogen diffusion [16].

In our work, Lotus glass, which is promised for advanced mobile displays [17], is used as substrate for IGZO deposition as well as for the glass surface studies. The contact angle of the glass surface after hydrogen plasma treatment was investigated to follow surface energy changes. Results shows that the glass surface becomes hydrophobic after hydrogen plasma and then gradually becomes hydrophilic again with time until reaching a constant low contact angle. This tendency suggests that hydrogen diffuses into the glass surface during the high-energy plasma treatment.

This hydrogen is then be released from the surface until it returns to a hydrophilic state.

2. Experimental Details

2.1 Thin Film Deposition by Sputter

Physical vapor deposition (PVD) is a technique used for thin film deposition. In PVD, pure source material is vaporized via high temperature evaporation, laser ablation, or plasma sputter bombardment, and then condenses on the substrate material to create a uniform thin film. It is a pure physical process and no chemical reactions are involved in the deposition process.

Sputter deposition is normally used for forming IGZO thin films on silicon or glass substrates.

The sputter system consists of a vacuum chamber, in which gaseous plasma is created. If the electrode is powered with dc, the electric field will accelerate a small number of free electrons in the chamber away from the target electrode, which is negatively charged (cathode). The chamber is filled with a low pressure of argon gas and the electrons will ionize the Ar atoms. These positive argon ions are then accelerated to the target cathode and strike the surface, dislodging target atoms and electrons into the chamber. The sputtered electrons will strike other neutral Ar atoms to form more positive argon ions to continue the process. Some electrons combine with Ar ions to form neutral atoms, releasing energy in the form of photons, giving the characteristic glow in the chamber (Figure 2). The pressure of chamber is typically between 1 and 100 mTorr.

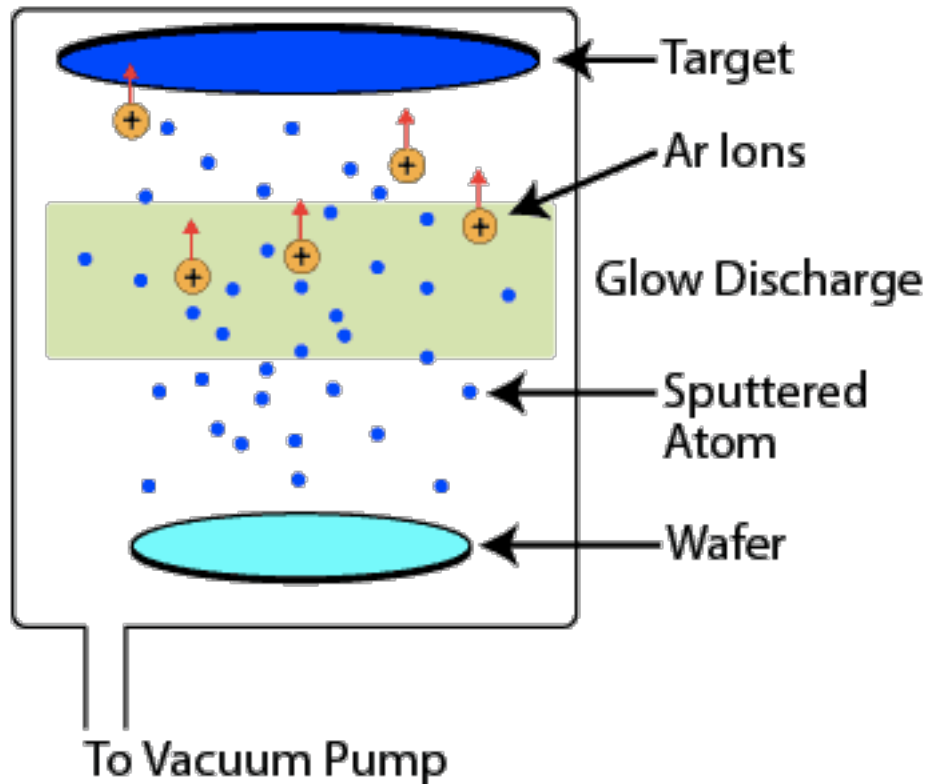


Figure 2 Sputter deposition system

There are some limitations for dc sputtering when the target material is highly resistive, such as for insulators or semiconductors. The cathode is supplied with constant negative voltage to sustain the plasma process, and the high resistivity of the target requires an unrealistic large voltage to maintain current through the target. The plasma process stops without a reasonable current.

For such targets, radio frequency (rf) voltage can be applied on the cathode to improve the deposition process. During the positive cycle of the rf voltage, electrons are attracted to the cathode to form a negative bias above the target. During the negative cycle, the Ar ions bombard the target yielding sputtered atoms and

electrons from the cathode. This avoids acceleration of the positive ions above the cathode when dc power is applied. RF power also enables the plasma process to work at lower pressure in the 0.5 to 10 mTorr range.

However, the positive ions not only bombard the target but also the substrate during rf sputtering, which can result in overheating and structure damage. To minimize this effect, the area of target is made small compared the substrate. In addition, the frequency of rf power must be high enough to prevent Ar ions from reaching the substrate during the negative voltage cycle, and is typically at 13.5 MHz. Deposition rates for rf sputtering are lower due to the lower ionization rate and the 50% duty cycle.

Magnetron sputter improves the deposition rate by increasing the efficiency of electron usage. A series of magnets with alternating polarity are placed behind the cathode. These magnets form a magnetic field above the cathode to trap the electrons. This prevents electrons from bombarding the substrate, and increases the electron gas density near the cathode to increase the ionization rate of Ar atoms by several orders of magnitude. Consequently higher plasma densities can be reached under relatively low pressures.

During sputtering, atoms eroded from the target are distributed in the chamber. Some will travel towards the substrate and are collected to form a thin film.

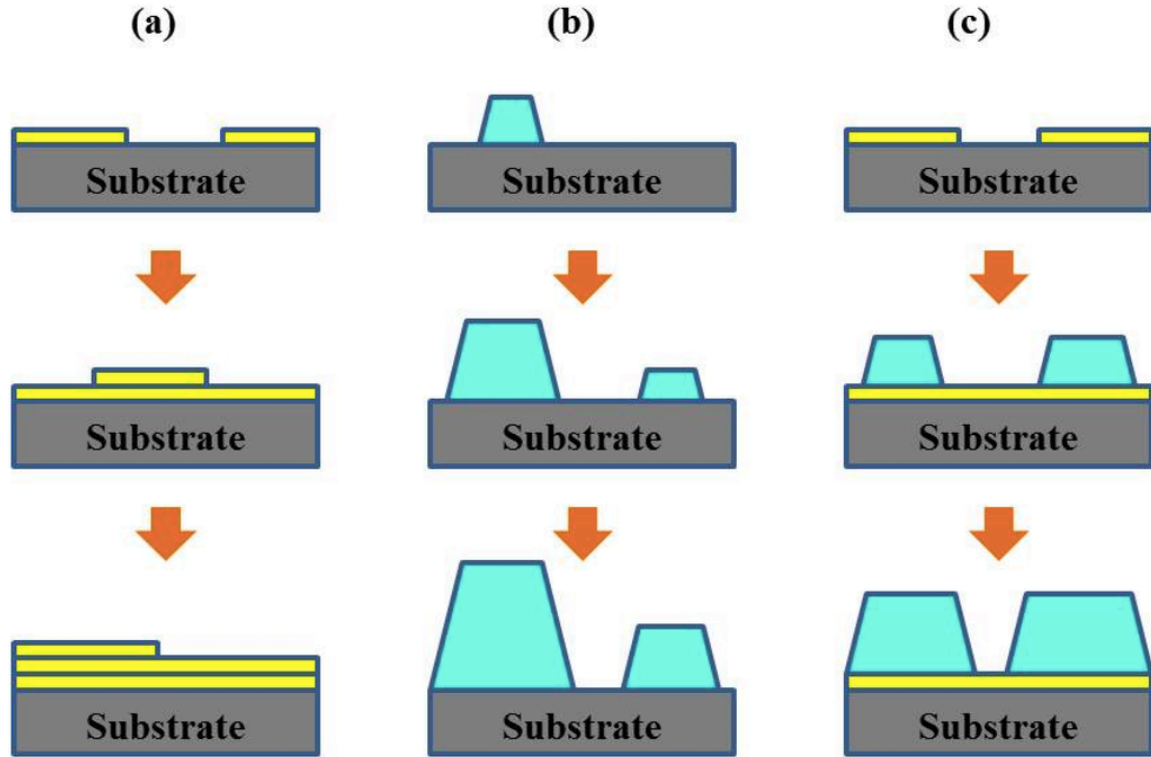


Figure 3 Schematic diagram of three modes of film growth: (a) Franck-Van der Merwe mode; (b) Volmer-Weber mode; (c) Stranski-Krastanov mode [18]

Figure 3 shows the potential growth processes on the substrate. Once target atoms or molecules arrive on the substrate, they are either absorbed onto the surface or are reflected back into the vacuum. The surface energy of adsorbed atoms is generally high and, to reach lower surface energies, the molecules diffuse along the surface to lower energy sites to form new bonds. During this surface diffusion, the adsorbed species will interact to form clusters. Once a cluster reaches a critical nuclei size, the cluster becomes thermodynamically stable and the surface energy is reduced due to the decrease of the surface area. Clusters smaller than this critical size are not stable and may desorb or be buried. The critical nuclei size depends on growth parameters including the substrate temperature and the film deposition rate.

If the interaction between the molecules and the substrate surface is very strong, the nuclei will tend to grow in a two-dimensional fashion and the thin film is formed in a layer by layer mode, which is called Franck-Van der Merwe mode (Figure 3a). If atoms or molecules have a greater affinity to bind together than to the substrate, the nuclei will tend to grow as three-dimensional islands, which is called Volmer-Weber mode (Figure 3b). The intermediate case between these two modes is called Stranski-Krastanov mode (Figure 3c), which can be described as initially forming a uniform thin film, which then becomes patchy as the interface interaction decreases. The nuclei tend to coalesce with each other to form large islands in order to reduce the surface energy. This process of nucleation and nuclei coalescence continues until the final film structure is formed.

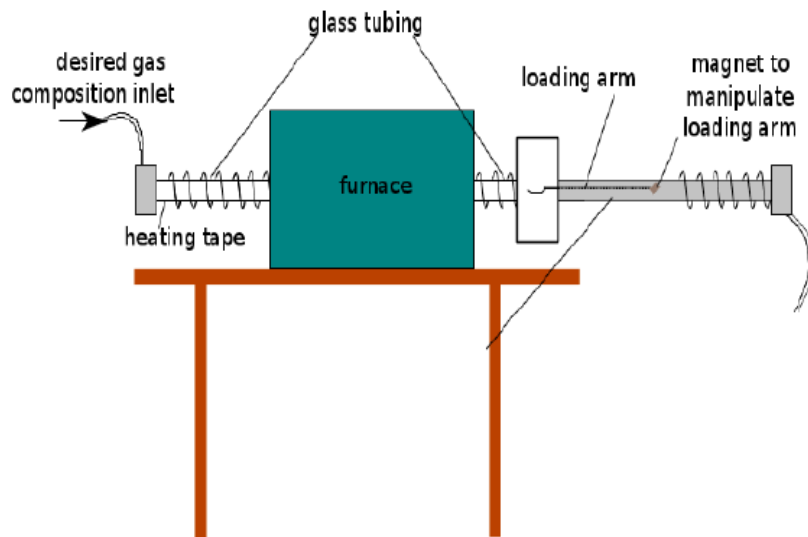


Figure 4 Typical wafer anneal furnace

After thin film deposition, it may be annealed in a UHV compatible furnace to adjust the electrical properties (Figure 4). The furnace contains a gas delivery system and the atmosphere can be controlled carefully during anneal.

2.2 Photolithography Process

In device fabrication process, photolithography is used to generate patterns onto the substrate. Patterns are transferred to photoresist layers on the substrate using UV light, the patterns are then transferred to the underlying material by etch or deposition processes. Photoresists are light-sensitive materials that are classified as two types: positive resists and negative resists. Positive resists are initially insoluble in a photoresist developer but becomes soluble when exposed to light. In contrast, negative resists are initially soluble but will become insoluble when exposed to light. Lithography tends to favor positive photoresist for high resolution and ease of use.

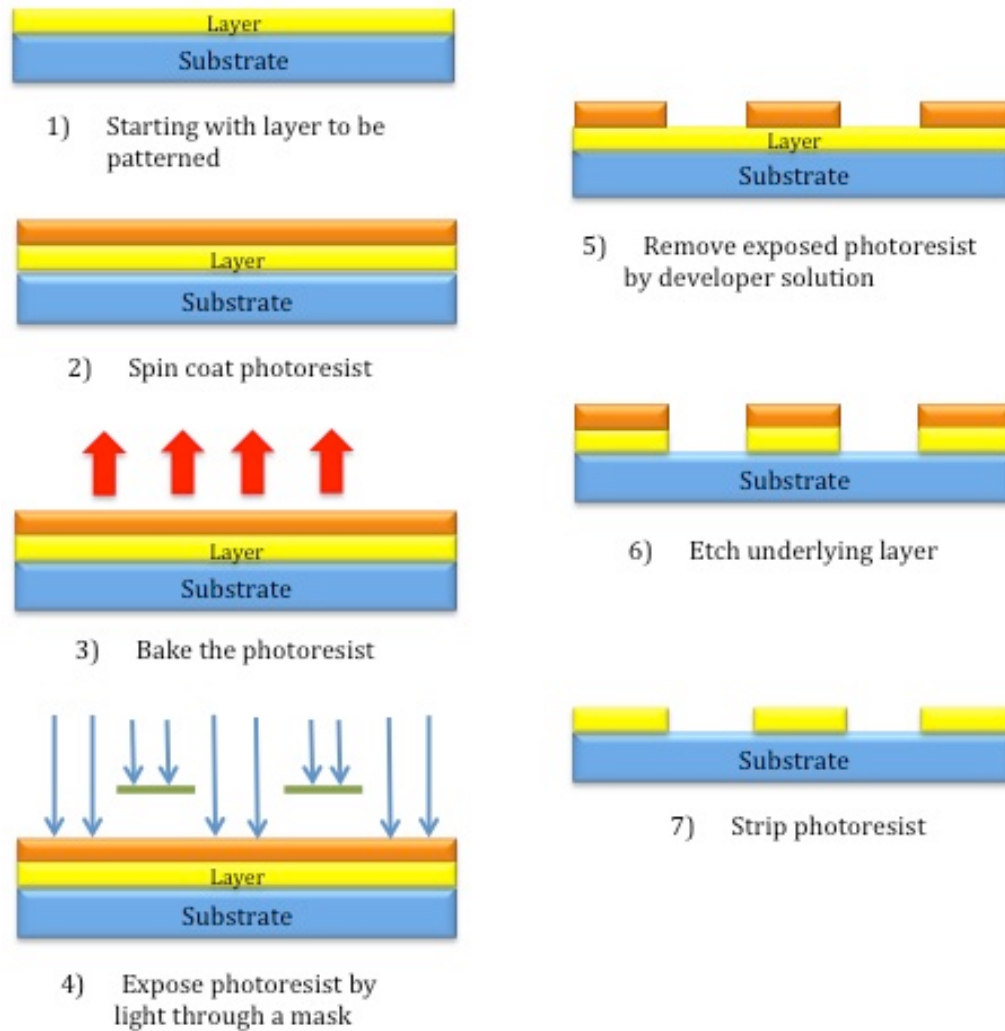


Figure 5 Steps of a photolithography process

The steps of a standard positive type photolithography process are shown in Figure 5. After the target layer is deposited on the substrate, photoresist is spin coated on the layer. To improve the adhesion of photoresist to surface, HMDS (hexamethyldisilazane) is normally used to prime the substrate surface. Then the sample is post-baked at a low temperature to evaporate remaining solvents from the spin-coat process. The wafer is then exposed to UV light through a photomask to change the solubility of the photoresist in the exposed region. A photoresist

developer is then used to remove the soluble resist; the remaining resist protects the target layer during etching of the underlying layer. Once the remaining photoresist is stripped off, the desired pattern is transferred to the underlying layer for subsequent processing.

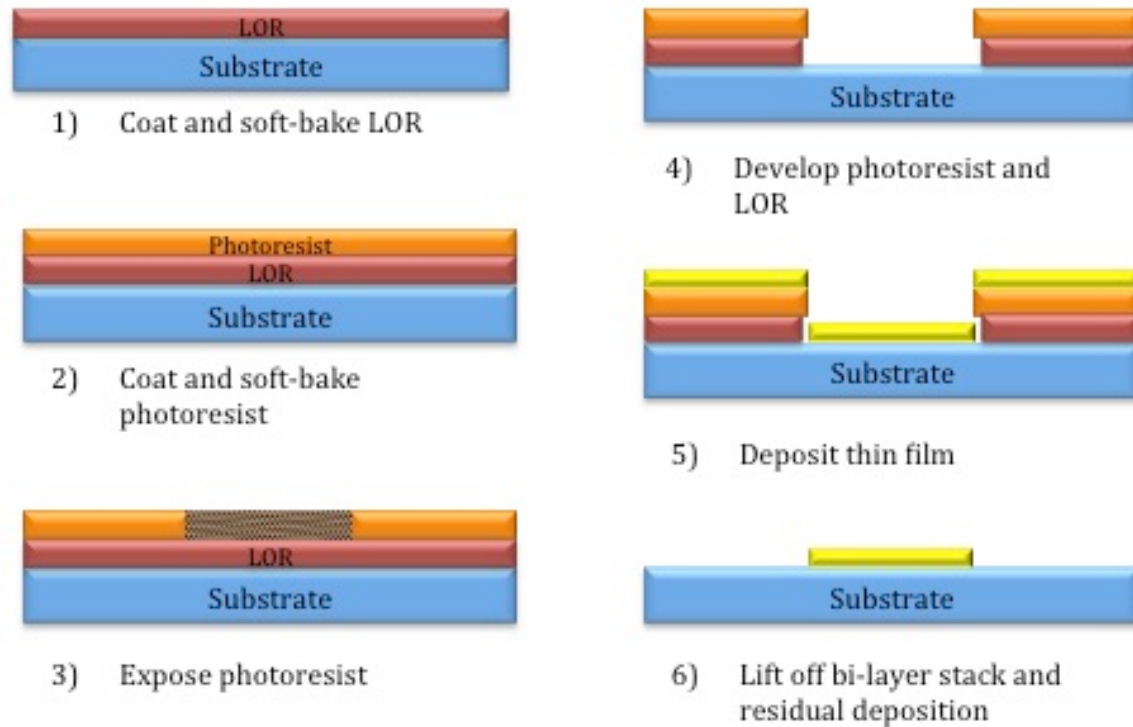


Figure 6 Steps of lift off process

A variant of this lithographic process is used to pattern evaporated films using a bilayer resist. This bi-layer process (Figure 6), using a lift off resist (LOR), is generally better controlled than alternatives such as the ammonia bake for resist reversal. An LOR resist is first spin coated and bake on the substrate followed by spin coating and baking of a normal photoresist. Then photoresist is exposed to UV light through a photomask to transfer the pattern. The LOR and photoresist in

exposed regions are dissolved by the developer. The target material is then deposited onto the substrate. The entire film is then placed in a resist stripper which removes the photoresist, LOR and the evaporated film. After this lift off, a thin film with the desired pattern is formed on the substrate.

The lift off process is normally used for metallization during IGZO device fabrication. Consequently the LOR is in direct contact with the IGZO surface. To explore the effect of the LOR resist on the IGZO surface, only the LOR 5A was spun on the IGZO and then stripped with MPR 1165 stripper.

2.3 PECVD

Chemical Vapor Deposition (CVD) is also widely used for film deposition. The CVD process involves precursor gases flowing into a vacuum chamber which then react to produce the desired material. Volatile by-products of the chemical reaction are removed from the chamber along with unreacted precursors.

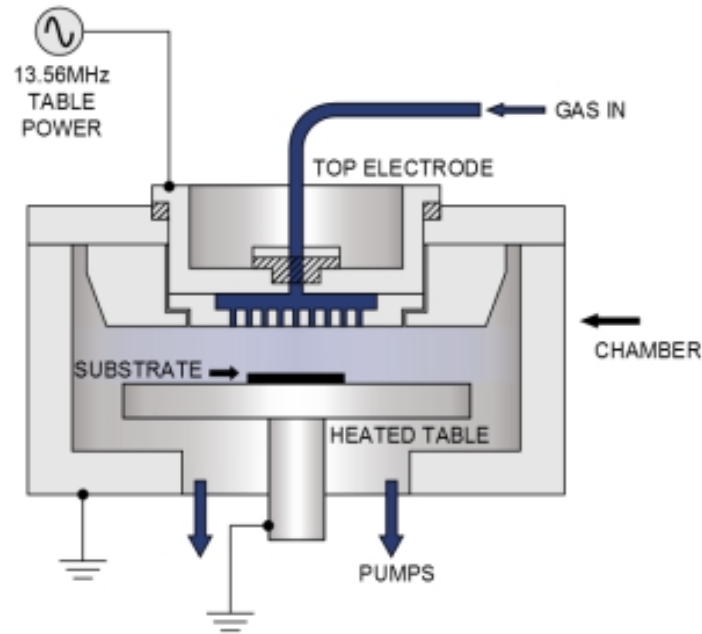


Figure 7 Structure of PECVD

Plasma enhanced chemical vapor deposition (PECVD) is used to improve the deposition rate at low temperature (Figure 7). The plasma process is similar to that involved in sputtering. Energetic electrons generated by the plasma help dissociate precursor molecules creating a large concentration of free radicals. Ions in the chamber bombard the reactor walls and the substrate. The deposited film is also exposed to ion bombardment, which helps with removal of surface contamination and improves the electrical and mechanical properties. High-density plasma can be also used to planarize the film or remove organic contamination from the surface, which improves the wettability of the surface [19].

2.4 Characterization

2.4.1 Contact Angle

Contact angle measurements are used to study the wettability of a surface. The contact angle is formed when a drop of liquid comes into contact with a solid surface and reflects the ability of the liquid spread out over the surface. Measurements of the angle can quantify changes in the surface chemistry and structure.

The contact angle is determined by properties of the liquid and solid, the intermolecular forces between liquid and solid, and the three phase interface properties. Normally the intermolecular forces consist of cohesion and adhesion. The cohesion forces, which cause liquid to resist separation, will force the liquid to form drops on a surface to minimize contact with the solid substrate. In contrast, the adhesion forces will lead the liquid to spread out on a surface and form a thin and uniform layer. The balance between these forces contributes to the final shape of a liquid drop on a solid surface.

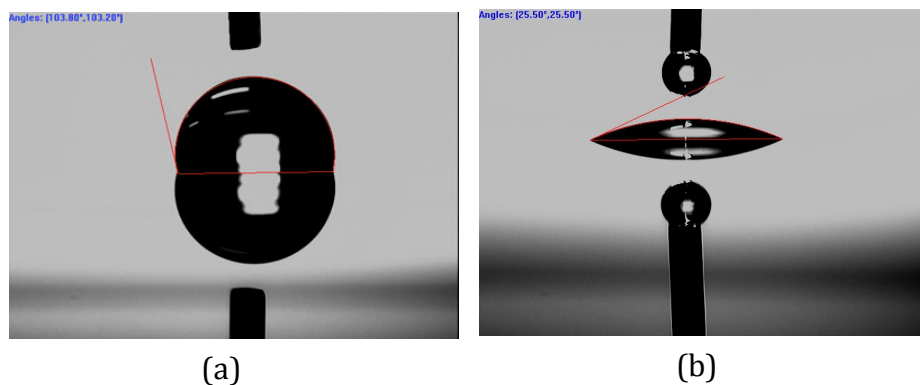


Figure 8 Contact angle of (a) a hydrophobic surface and (b) a hydrophilic surface

In this work, I used deionized water (DI) as the liquid to measure the wettability of the target surfaces. Figure 8 shows a hydrophobic surface and a hydrophilic surface formed by DI water with different surfaces. A large contact angle indicates strong cohesion force of the liquid molecules relative to the adhesion force. A smaller contact angle indicates stronger adhesion forces, which leads to more interaction between liquid and solid.

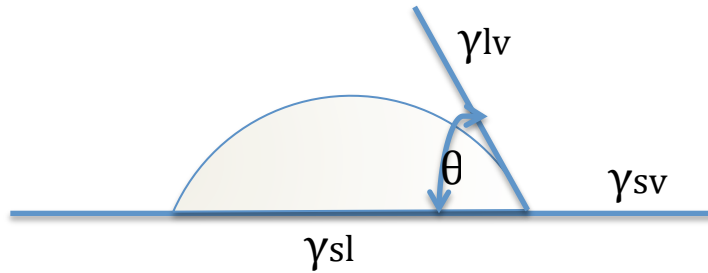


Figure 9 Definition of the contact angle formed by liquid drop and solid surface

Figure 9 shows the definition of contact angle. According to Young's equation [20], the contact angle of a drop of liquid on a substrate of solid is determined by the equilibrium of three surface tensions.

$$\gamma_{sv} - \gamma_{sl} = \gamma_{lv} \cos \theta$$

where γ_{sv} represents the surface tension at the interface of the solid and vapor; γ_{sl} is the surface tension at the interface of the solid and liquid; γ_{lv} is the surface tension at the interface of liquid and vapor; and θ is the contact angle formed by the drop.

2.4.2 4-Point Probe Measurement

Resistivity is an important parameter of semiconductor materials that is related to the impurity concentration. The 4-point probe measurement was used to determine the sheet resistance and bulk resistivity of IGZO layer before and after LOR treatment.

During the 4-pt probe measurement, four thin wire probes were placed colinearly to make contact with the surface of the sample as shown in Figure 10.

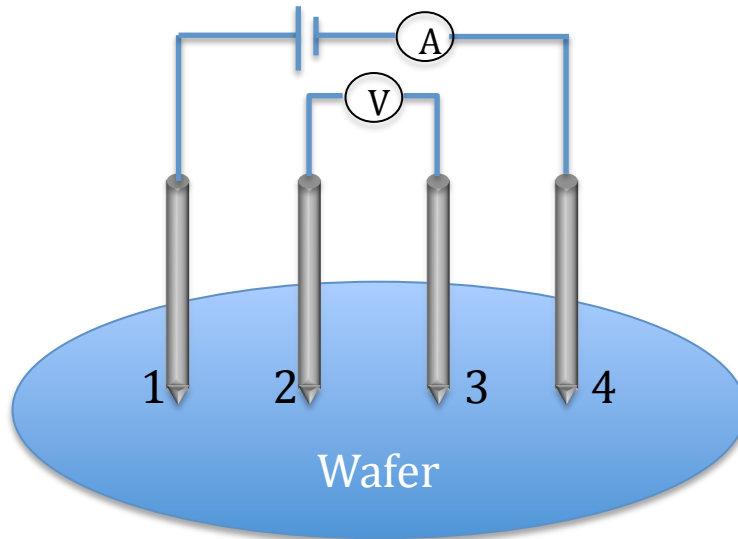


Figure 10 4-point probe

Current is supplied via connections 1 and 4 and voltage is measured between the connections 2 and 3. Contact resistance is eliminated by separating the current and voltage sensing electrodes. The current was swept over a range to accurately determine the resistance. The resistance of samples varied by several orders of magnitude, requires currents from 200 μA to 20 nA. The spacing between the 4 probes was equal and the sample layer thickness was less than half of the probe spacing distance. The sheet resistance was hence calculated as

$$R_s = 4.532 \times \frac{V}{I} \times \text{Edge correct}$$

where the R_s is sheet resistance, V is measured voltage and I is current supplied.

The edge correction is only required for small samples and was unnecessary in this work [21]. The resistivity can be calculated as

$$\rho = R_s \times t$$

where ρ is the resistivity and t is the thickness of the film.

2.4.3 Atomic Force Microscope

Atomic Force Microscopy (AFM) was used to study the surface structures of plasma processed glass substrates. Oxygen plasma treated and hydrogen plasma treated commercial glass samples were measured to determine the surface roughness. Tapping mode was used to scan a square area with 500 nm sides and the mean square roughness (R_q) was measured.

3. Results and Discussions

3.1 IGZO Film Surface

3.1.1 Storage Conditions

During fabrication of IGZO thin film transistors, it was discovered that devices with no back passivation deteriorated within a short time period (days). To understand these changes, we investigated the effect of the storage environment on the IGZO surface.

Lotus glass wafers (obtained from Corning) were deposited with IGZO and stored in varying environment. IGZO was sputter deposited in a 10% O₂/90% Ar ambient with substrates held at 350°C with 150 W rf power for 15 min. The contact angle for as-deposited IGZO was 14.2° with variation less than 0.5°. The wafers were then treated in four different ways: a) stored in a vacuum desiccator; b) stored in cleanroom ambient air; c) spin coated with photoresist primer and S1813 photoresist, then baked at 90°C for 5 min and stored in cleanroom ambient air; d) spin coated with LOR using a two-part spin process (500 RPM, 100 RPM/s ramp, 5 s followed by 3000 RPM, 500 RPM/s, 30s), then baked at 180°C for 5 min and stored in cleanroom ambient air. For each treatment, wafers were both stored in clear wafer trays and opaque wafer trays for three days. Prior to measurements, wafers coated with S1813 were immersed in acetone, followed by IPA and deionized water. Wafers coated with LOR were immersed in MPR 1165 solvent for 20 min, followed

by rinsing with acetone, IPA and deionized water to remove the resist. The contact angles of IGZO surfaces were then measured using the VCA Optimal tool.

Table 2 Contact angle of IGZO samples under different storage conditions

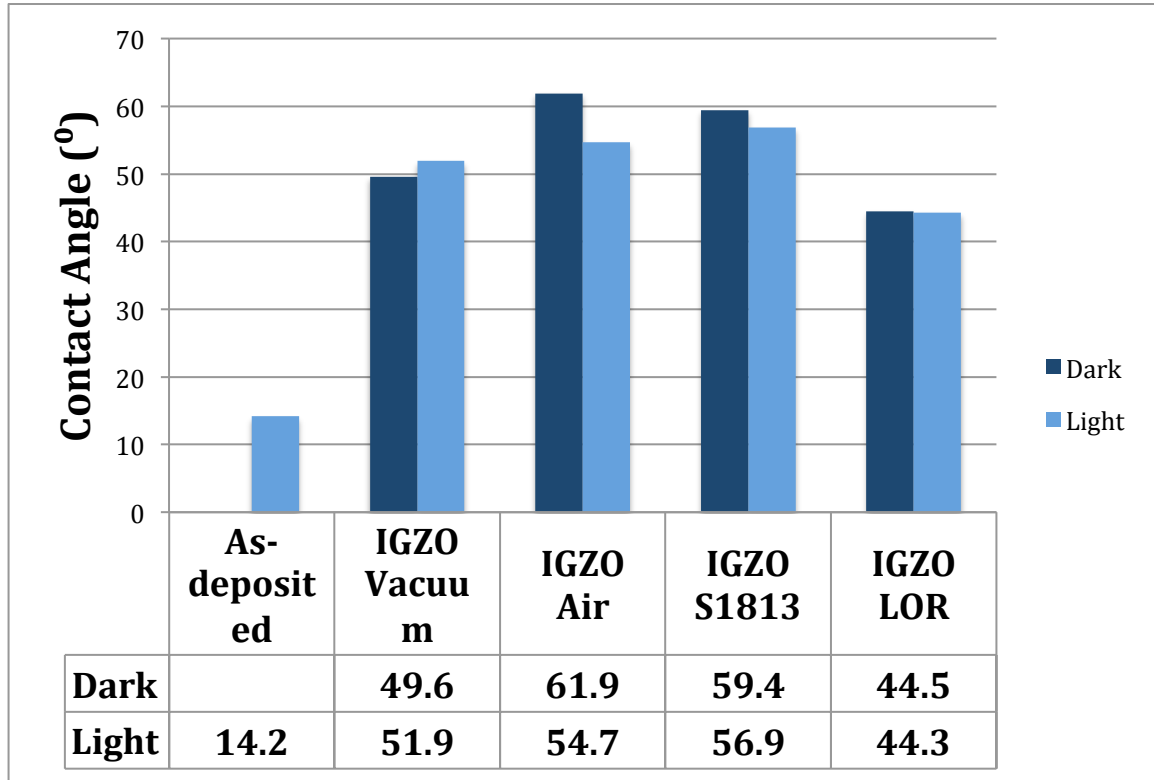


Table 2 shows results of the contact angle measurements. Wafers stored directed in vacuum showed minimal differences between light and dark, but do still exhibit substantial change from the initial state. For IGZO wafers stored simply in cleanroom air, there is a significant difference between samples stored in dark or in ambient light. This effect is likely due to photochemical induced changes from organic contaminants in the cleanroom environment. The S1813 and LOR treated wafers showed comparable changes due to the chemical resist, but no light induced effects. The results indicate significant surface modification based on surface

treatments even after identical final organic cleans. In all cases, storage resulted in surface becoming more hydrophobic.

3.1.2 Surface Changes with Time

The bare IGZO surface and IGZO coated with LOR 5A were monitored by contact angle measurement as a function of time. All wafers were stored in clear wafer trays in cleanroom ambient air.

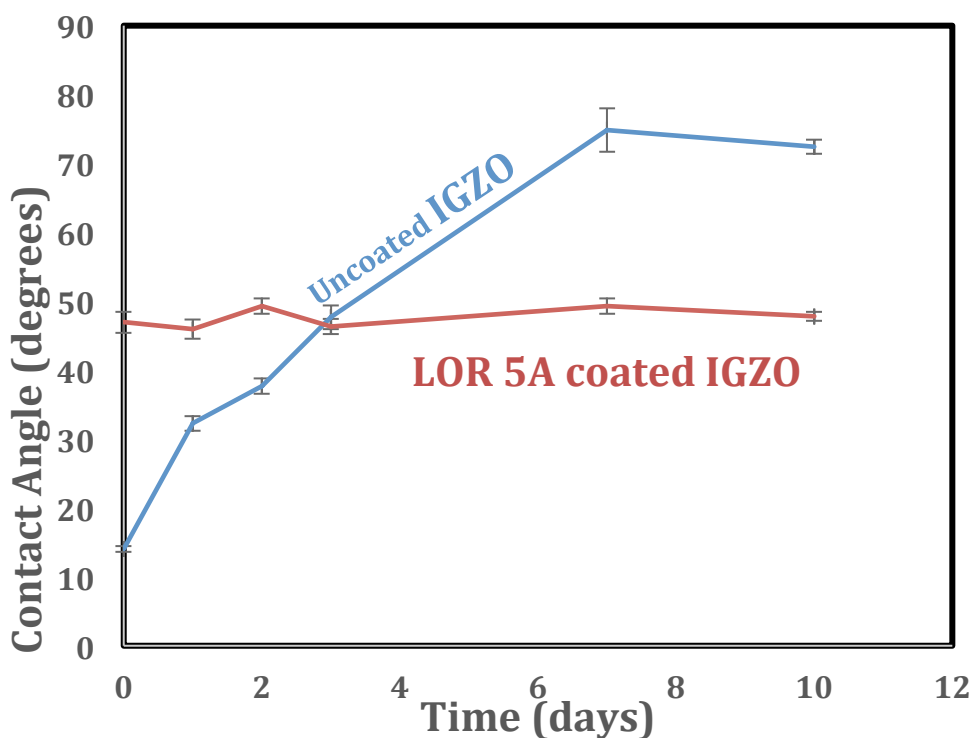


Figure 11 Contact angle changes with storage time for uncoated IGZO sample and LOR 5A coated IGZO sample. Uncertainties are based on the standard deviation of five measurements on each sample.

As shown in Figure 11, untreated, as-deposited a-IGZO films are hydrophilic immediately and exhibit a steadily increasing in contact angle with time. This suggests that the adsorption of environmental contaminants decreases the surface

energy. In contrast, samples treated with LOR 5A exhibited an almost immediate hydrophobic change with an increased contact angle. The contact angle was constant with time then, suggesting permanent surface modification due to the LOR 5A.

To conclude, uncoated IGZO surfaces gradually became hydrophobic due to organic contamination even in a cleanroom environment. Both S1813 and LOR resists modify the surface of IGZO. The effect is not the same for both resists, suggesting some chemistry dependence. Surface changes with resist appear to be immediate with no “diffusional” effect that would increase with time.

3.1.3 Effect of LOR Treatment to IGZO Thin Film Conductivity

Contact angle measurement showed surface energy modification by LOR treatment. To further explore the impact of LOR 5A on a-IGZO films, sheet resistances of as-deposited a-IGZO films of various thicknesses were measured by Kathryn Roach in our subgroup. The sheet resistances of as-deposited a-IGZO films were measured using a 4-point probe. LOR 5A was then spun onto the a-IGZO films and baked on a hot plate at 180°C for 5 minutes in air. The LOR 5A was removed by immersing films in MPR 1165 solvent overnight to ensure removal of the resist, followed by rinsing with acetone, IPA and DI water. The sheet resistances of the resulting bare a-IGZO films were measured.

Table 3 Sheet resistance for IGZO film before and after LOR treatment

IGZO thickness	As-deposited [Ω/\square]	Post-treatment [Ω/\square]
33 nm	3,100,000	30,000
50 nm	54,000,000	83,000
67 nm	9,300,000	320,000
83 nm	43,000,000	1,100,000

The as-deposited sheet resistances and the post-LOR sheet resistances are shown in Table 3. For all of the investigated film thicknesses, the high sheet resistance measured for as-deposited samples indicated insulating films. However post-treatment of samples with LOR reduced the sheet resistance by up to two orders of magnitude. IGZO films clearly exhibit enhanced doping due to exposure with LOR 5A.

3.1.4 LOR Post-baking Temperature

The bake temperature for LOR 5A was 180°C, which is high enough to potentially diffuse H⁺ or other ions into the IGZO films. Contact angle and 4-point probe measurement were investigated on LOR treated IGZO surface as a function of the bake temperature to further understand the doping. Glass substrates were deposited with 50 nm IGZO film by sputter deposition (10% O₂/90% Ar, 350°C

substrate temperature and 120 W rf power). The contact angle of the as-deposited IGZO surface was 14.2° and the sheet resistance was $1.4 \times 10^8 \Omega/\square$ with an estimated carrier concentration of $9.2 \times 10^{14} \text{ cm}^{-3}$. The IGZO surface was spin coated with LOR 5A resist. Wafers were then baked on a hot plate at varying temperatures for 5 min. After cooling down to room temperature, the wafers were immersed in MPR 1165 solvent for 20 min to remove the LOR 5A. Contact angle and sheet resistance were then measured. The carrier concentration was estimated using an IGZO mobility of $10 \text{ cm}^2/\text{Vs}$.

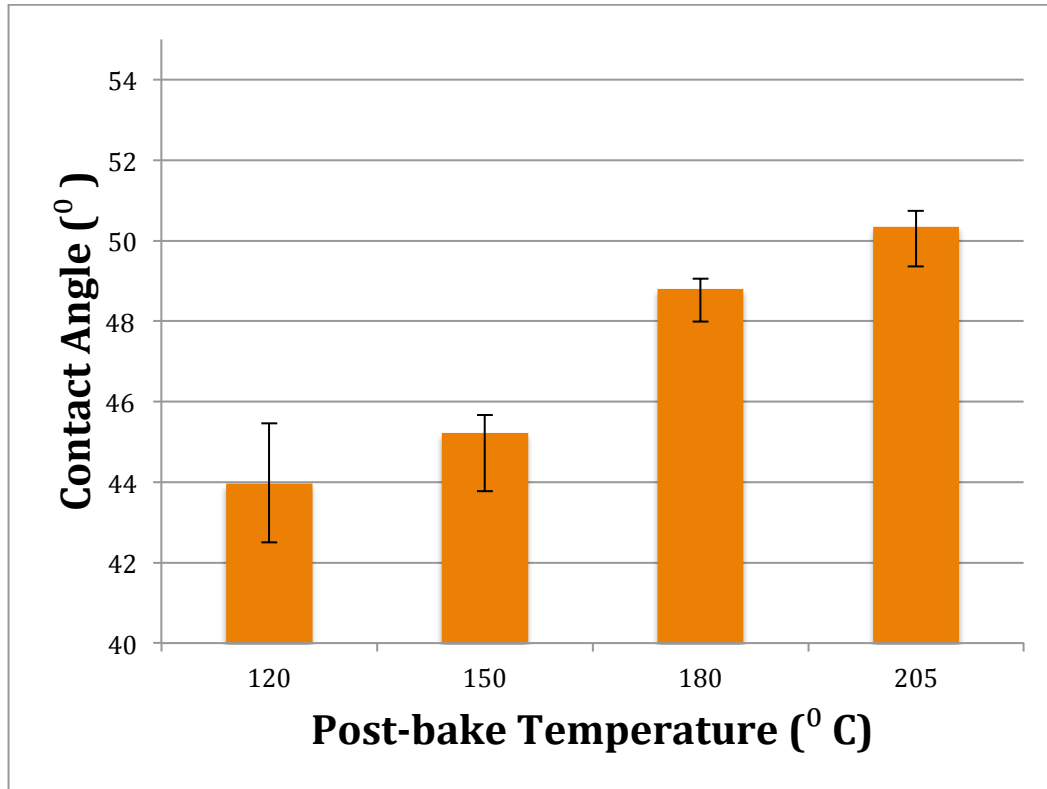


Figure 12 Contact angles of IGZO samples after LOR treatment at different temperatures. The as-deposited contact angle was 14.2° .

Figure 12 shows the increasing trend of contact angle with increasing bake temperature from 120°C to 205°C. The continued increase in contact angle with temperature suggests either a diffusion or direct chemical reaction between the IGZO and the LOR 5A resist.

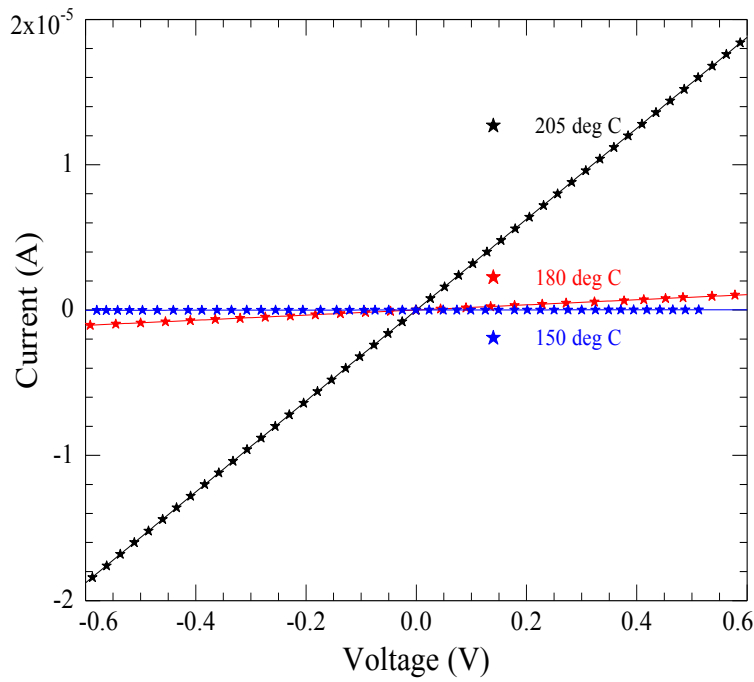


Figure 13 Current sweep for IGZO samples after LOR treatment with different bake temperatures

The results of 4-point probe measurement after LOR treatment at different bake temperatures are shown in Figure 13. The conductivity increases dramatically with increasing bake temperature.

Table 4 Effect of LOR bake temperatures on IGZO properties

Post-bake Temperature ($^{\circ}\text{C}$)	As-deposited	150	180	205
Contact angle ($^{\circ}$)	14.2	45.2	48.8	50.3
Sheet resistance (Ω/\square)	1.4×10^8	1.4×10^8	2.6×10^6	1.4×10^5
Resistivity ($\Omega \cdot \text{cm}$)	680	720	13	0.72
Carrier Concentration (cm^{-3})	9.2×10^{14}	8.7×10^{14}	4.8×10^{16}	8.6×10^{17}

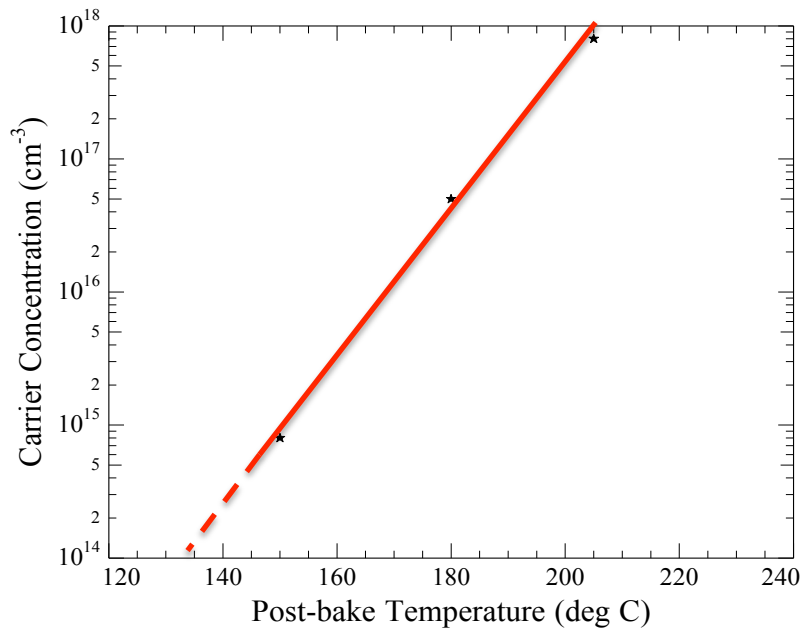


Figure 14 Carrier concentration of IGZO film after LOR treatment at different temperatures

The calculated sheet resistance and carrier concentrations are shown in Table 4 and Figure 14. The increase of carrier concentration at 180°C and 205°C indicates an increased doping above a critical temperature, which is consistent with the results of the contact angle measurements.

3.1.5 Film Conductivity after Annealing

Thermal anneals alone in a low p_{O_2} environment will also induce carriers in IGZO films. While anneal temperatures are generally higher ($>350^\circ\text{C}$), the effect of low temperature was also investigated.

50 nm IGZO thin film was sputter deposited on Lotus glass followed by annealing in an UHV compatible furnace with nitrogen gas flow at 350°C for 30 min. The annealed sample was then measured using the VCA Optimal (contact angle) and 4-point probe (carrier density).

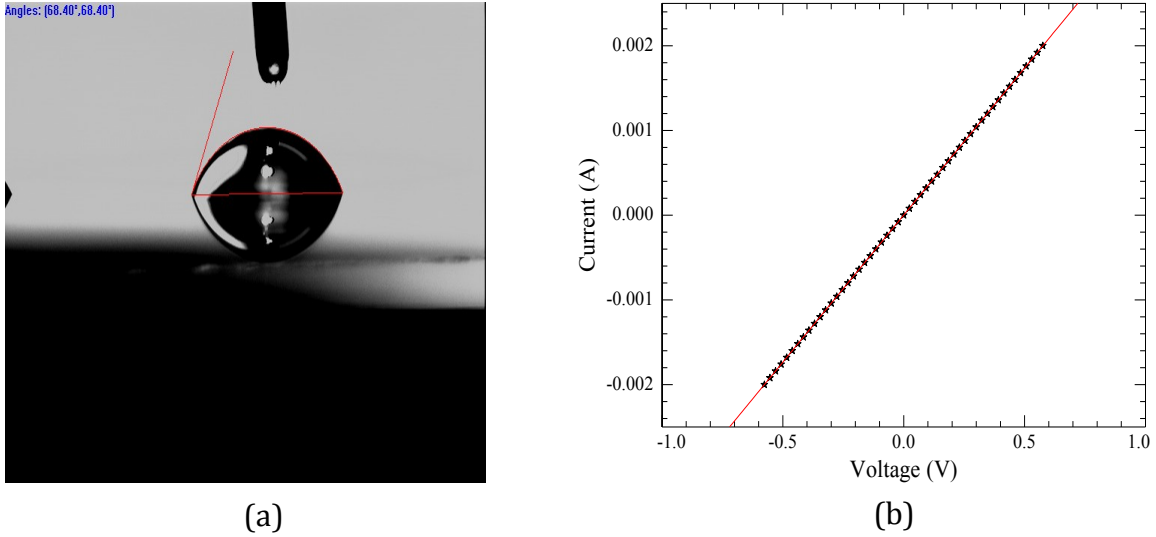


Figure 15 (a) Contact angle (b) current sweep curve for 350°C annealed IGZO sample

Figure 15 shows the contact angle and 4-point probe measurement of this annealed IGZO sample. The contact angle was 68.4° with a sheet resistance of $1300 \Omega/\square$. This contact angle is dramatically higher than any of the previous measurements

suggesting significant surface modification in the UHV furnace. Nitrogen annealing indeed decreased the sheet resistance by 5 orders of magnitude with carrier concentrations approaching 10^{19} cm^{-3} .

The IGZO thin film was deposited with reactive sputtered Ar and O_2 , leading to low oxygen vacancy concentrations. The deposited film hence shows insulating behavior since carrier concentration is proportional to the oxygen vacancy concentration [22]. Nitrogen anneals, result in highly conductive (metallic like) IGZO films, presumably due to a higher carrier concentration from the increased oxygen vacancies [23].

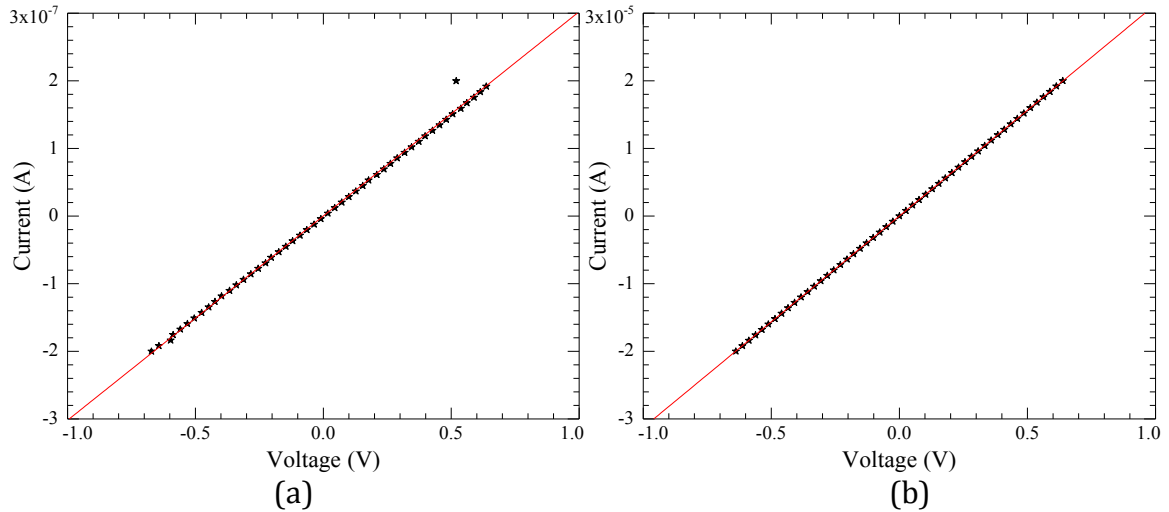


Figure 16 Current sweep curve of IGZO sample for (a) annealed with N_2 at 205°C for 5 min (b) LOR treatment with 205°C baking for 5 min. The current scales in the two cases differ by a factor of 100.

IGZO samples were then annealed under nitrogen at 205°C for 5 min to compare thermal and LOR effects (Figure 16). The sheet resistance measured after the nitrogen anneal was $1.5 \times 10^7 \Omega/\square$, with an estimated carrier concentration of $8 \times 10^{15} \text{ cm}^{-3}$. This is nearly 2 orders of magnitude lower than observed in LOR 5A treated IGZO sample with a 205°C bake. This indicates that the effect from the LOR is not simply thermal but must be due to chemically induced changes in the IGZO films. Because the doping occurs at relatively low temperature, we suggest that the doping is due to hydrogen diffusion into the IGZO rather than an increase of oxygen vacancies.

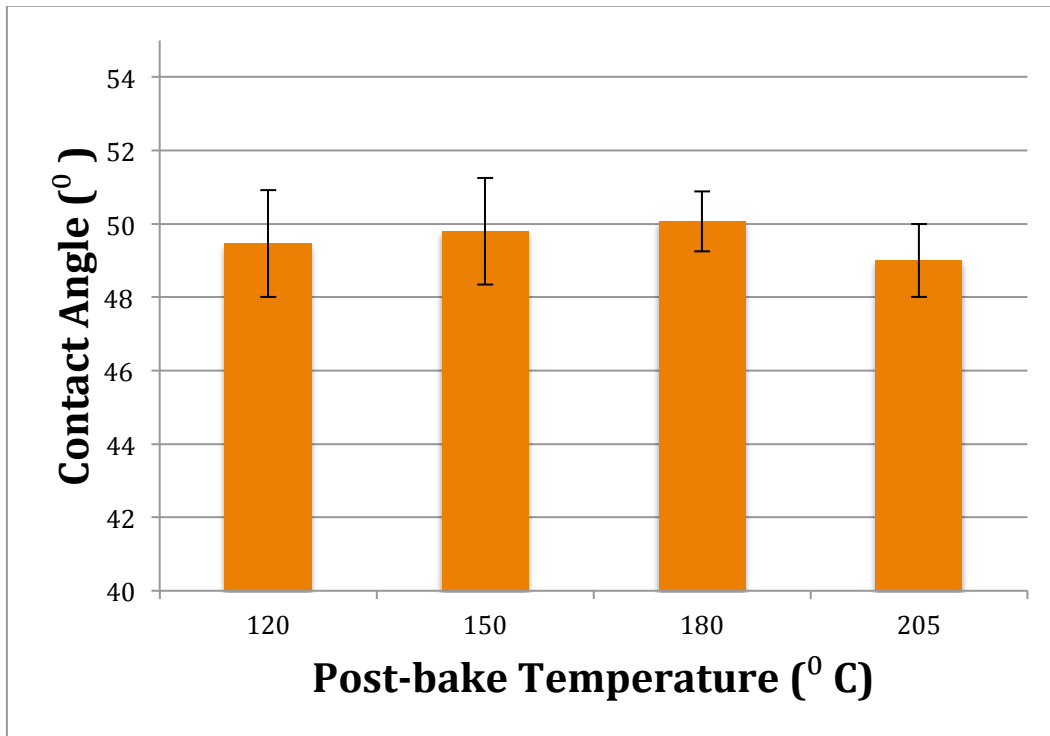


Figure 17 Contact angle of IGZO samples annealed in N_2 at 350°C followed by post anneal with LOR at different temperatures

Table 5 Estimated carrier concentration for samples treated with LOR 5A after a 350°C furnace N₂ anneal

Post-bake Temperature (°C)	No LOR treat	120	150	180	225
Sheet resistance (Ω/\square)	1300	1100	1200	1000	1300
Carrier Concentration (cm ⁻³)	0.96×10^{20}	1.1×10^{20}	1.1×10^{20}	1.2×10^{20}	0.98×10^{20}

LOR treatments at different bake temperatures were also applied to nitrogen annealed IGZO samples. Though the contact angle decreases compared with sample with no LOR treatments, the contact angle after LOR treatment is nearly independent of the bake temperature. This is not surprising (Figure 17) because the removal process may also remove some surface contaminants adhered during nitrogen anneal process. The sheet resistance and estimated carrier concentration remain essentially constant and independent of the LOR bake temperature (Table 5). After an N₂ anneal that has dramatically increased the carrier concentration, small additional doping from LOR does not have a significant effect.

3.1.6 Discussion

The effect of LOR processing on IGZO is temperature dependent, but more complicated than thermal doping. One component of LOR 5A is Poly(methyl methacrylate) (PMMA), an acid-based polymer. We proposed that, during high

temperature baking, the acidic behavior induces mobile hydrogen ions to diffuse into the surface of the IGZO.

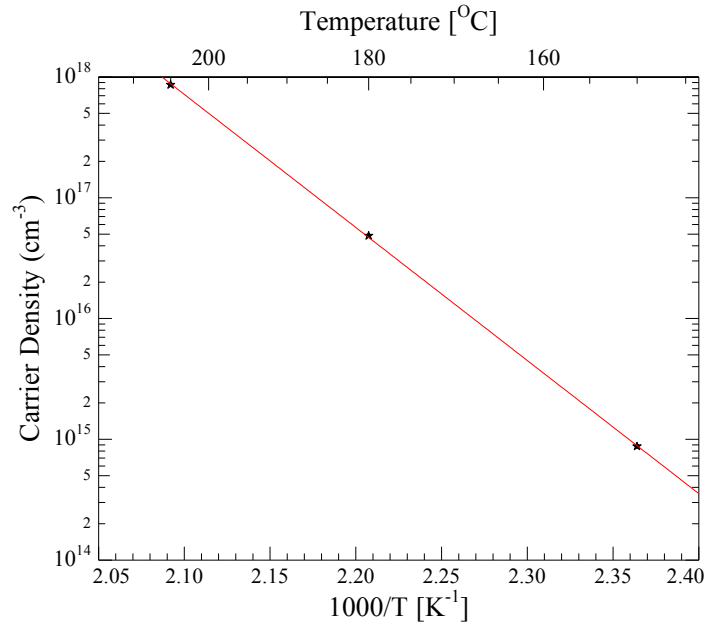


Figure 18 Carrier density as a function of the inverse LOR bake temperature

The activation energy, estimated from the carrier density and bake temperature as shown in Figure 18, is 2.2 eV. This is in the typical range for decomposition of chemical bonds in polymers such as PMMA [24]. It is likely that decomposition of PMMA, or another organic molecule in the LOR, releases hydrogen ions that diffuse into the IGZO and act as dopants.

3.2 Glass Surface

3.2.1 PECVD Treated Glass Surface

Glasses are the conventional substrate for thin film device fabrication. The effect of hydrogen plasma processing on the glass surface was explored to better understand and monitor changes in the glass behavior.

Lotus glass wafers were cleaned with RBS 35 detergent at room temperature for 5 min, following by rinsing with acetone, IPA and deionized water. The contact angle of the clean glass surface was around 25° (figure 20a). The glass wafers were then treated for 5 min in an oxygen plasma using the Glen 1000 tool. After the O_2 plasma clean, the surface became extremely hydrophilic with a contact angle of around 5° (figure 20b). The oxygen radicals and the vacuum UV exposure during the plasma clean helps to break the chemical bonds of surface organic contaminates, which then react with oxygen radicals to form lower weight hydrocarbons. These products are evacuated from the chamber with the gas flow.

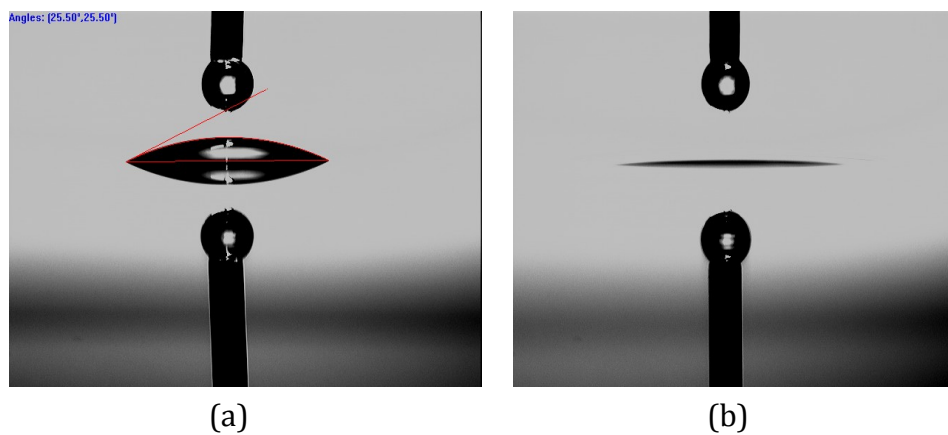


Figure 19 Contact angle of glass (a) before oxygen plasma (b) after an oxygen plasma clean

The wafers were then loaded into the Oxford PECVD chamber. The wafer chuck was held at 350°C and the chamber pressure during processing was 1900 mTorr argon. Then wafers were treated using the standard hydrogen plasma recipe (2000 mTorr chamber pressure, 300 W rf power. Gas flow rate: H₂: 90 sccm; Ar: 45 sccm) with a H₂/Ar ratio of 2:1 for varying times. Contact angles of the wafer surfaces were measured then using the VCA Optimal tool.

Table 6 Contact angle of glass surface after hydrogen plasma treatment

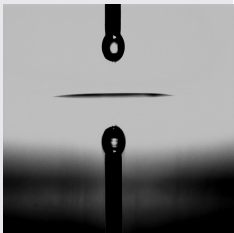
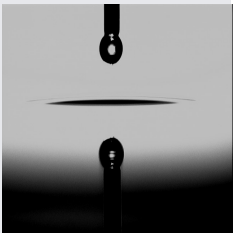
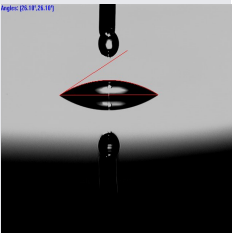
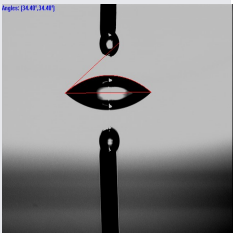
Hydrogen plasma time	0 min	5 min (H ₂ , no plasma)	1 min	5 min
Contact Angle	5.5° 	6.5° 	26.1° 	34.4° 

Table 6 shows the contact angles after different treatment conditions. To ensure that effects were due to the plasma, the change induced by just the H₂ flow was first measured. With no plasma, the surface remained extremely hydrophilic with neither the gas nor the chamber contaminating the surface. With the hydrogen plasma, the surface quickly become more hydrophobic reaching a contact angle of 34° after 5 minutes.

The contact angle was followed with time to determine if the changes were permanent. Contact angles were measured on different areas on a single wafer and wafers were stored in clear boxes in the cleanroom during multiple measurements.

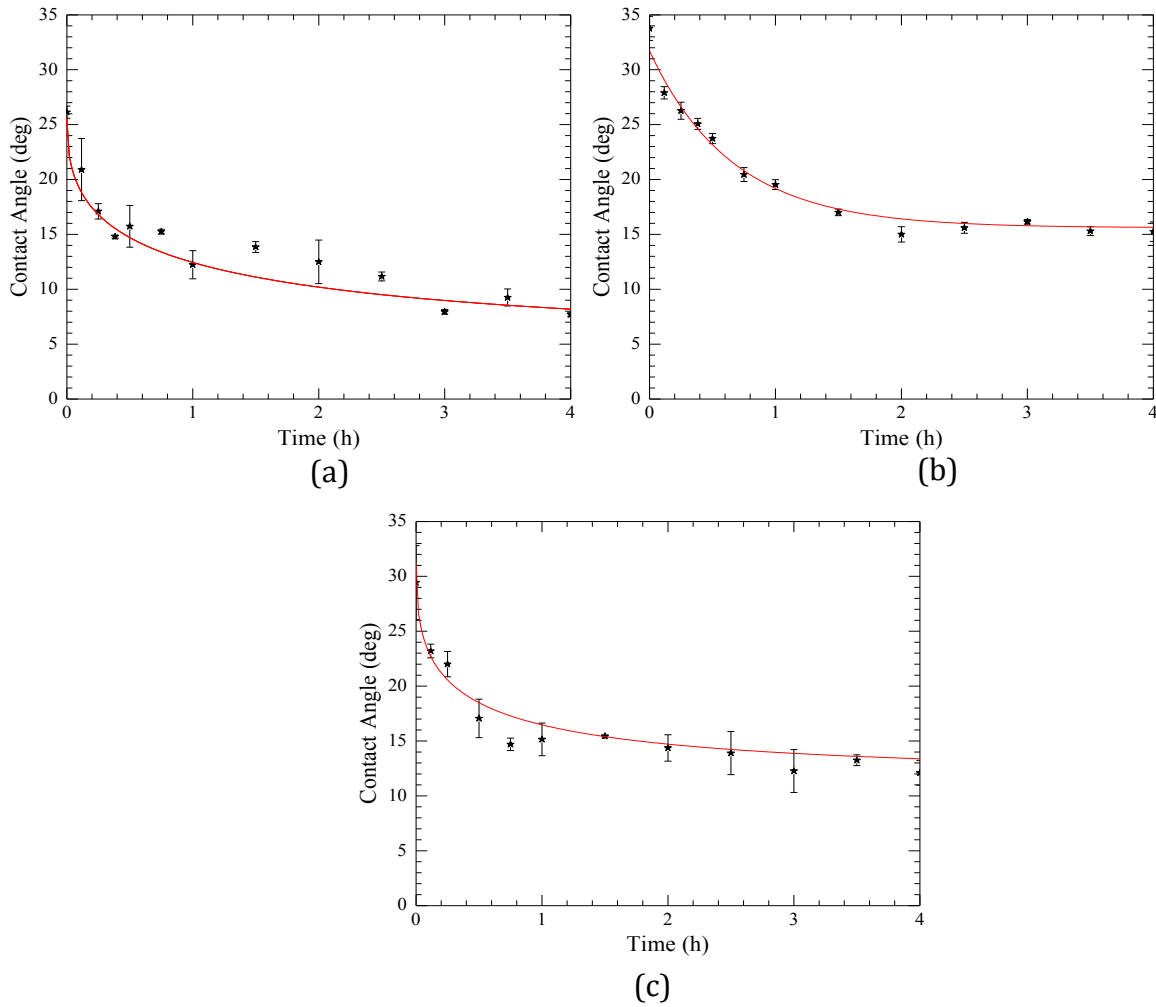


Figure 20 Contact angle changes with time after hydrogen plasma treatment for (a) 1min; (b) 5 min; (c) 10 min

Figure 20 shows contact angle changes with time after hydrogen plasma treatment and fit exponentially. The contact angle dramatically increased immediately after

the hydrogen plasma, then decreased gradually until reaching a final level near 10^0 . This tendency was also observed for samples exposed to the hydrogen plasma without an oxygen plasma clean, eliminating the potential of a delayed effect from the oxygen plasma.

We propose a potential mechanism involving hydrogen diffusion into the glass surface. Although hydrogen diffusion in glass is very slow even at 350°C , the activated hydrogen ions in the plasma could diffuse into the near surface during the plasma treatment. Later, the hydrogen is slowly released from the near surface resulting in the increased hydrophilicity of the surface with time.

3.2.2 Surface Roughness

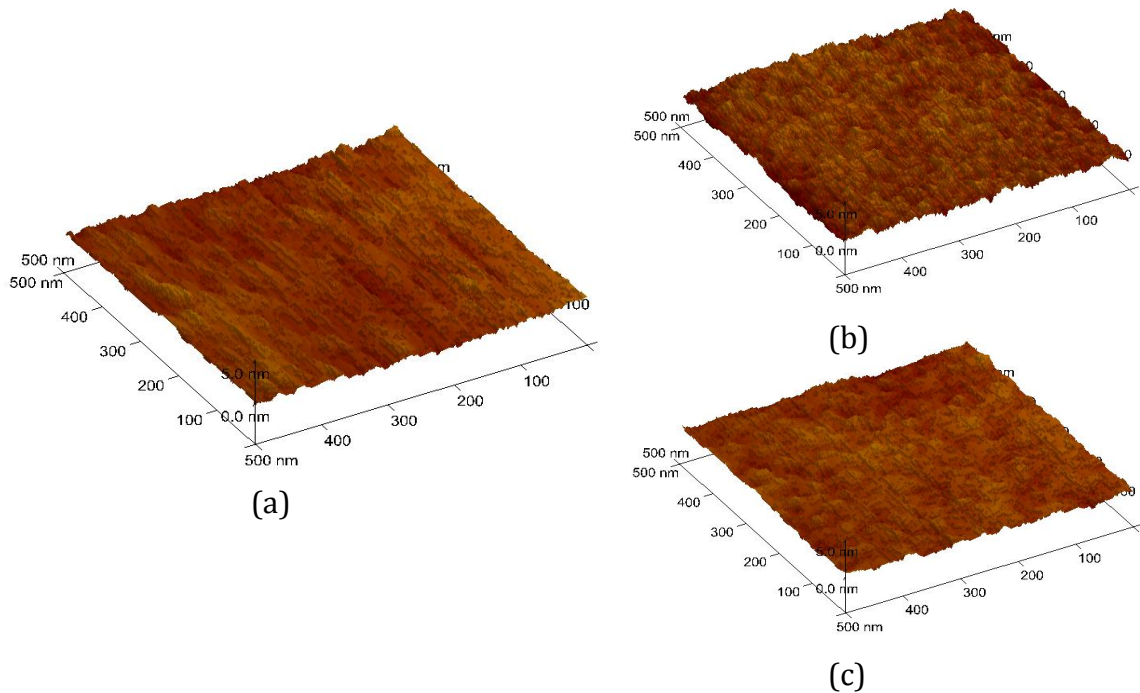


Figure 21 Surface roughness of glass surface (a) after solvent cleaning; (b) after oxygen plasma; (c) after oxygen plasma and hydrogen plasma

Surface energies are also known to be affected by surface roughness. Plasma processing can also etch the surface and hence changes in the surface morphology. To explore this effect, AFM was used to compare surface before and after plasma processing. Figure 21 shows the surface roughness for glass wafers with different treatments. For glass wafers cleaned with solvent, and subsequently with oxygen plasma, the roughness was 0.288 nm and 0.358 nm respectively. For glass wafers treated with the hydrogen plasma after the oxygen plasma clean, the roughness was 0.364 nm. While the oxygen plasma caused a very small increase in surface roughness [25], there was no measurable difference after the hydrogen plasma. This result indicates that the hydrogen plasma effect on the glass surface is not due to morphological changes in the surface layer, but rather must be a result of chemical changes or hydrogen diffusion during plasma treatment.

4. Conclusions

The effect of the photographic lift off process on IGZO thin film deposited on glass substrates has been studied using contact angle measurement and 4-pt resistivity measurement. IGZO is sensitive to the storage environment. Result shows that contaminants from air adhere to IGZO surface rapidly modifying the surface energy. The contact angle of the IGZO surface was investigated as a function of time and showed that uncoated IGZO surfaces gradually became hydrophobic. Spin coating of LOR 5A resist resulted in nearly immediate increases in the contact angle, which was permanent with no further increase with time.

The LOR process also impacted the sheet resistance of the IGZO layer, which was correlated with surface energy changes. LOR coated IGZO wafers were baked at various temperatures. The carrier concentrations, estimated by sheet resistance measurements, increased with the bake temperature, indicating that the doping effect occurs above a critical temperature. This behavior was similarly observed in the contact angle measurements.

The effect of nitrogen anneals on the IGZO thin film was compared with the LOR effect. The increase of carrier density by LOR is nearly 100 times larger than a similar thermal anneal, which indicates the effect from LOR is not simply thermal. We suggest the increased carrier concentration is due to hydrogen-based doping from the LOR resist rather than an increase in the oxygen vacancy concentration.

At high temperatures, nitrogen annealing significantly increase carrier concentration by 5 orders of magnitude. After such anneals, LOR processing did not significantly modify the conductivity further.

Hydrogen diffusion into glass surface during plasma processing was also studied for “Lotus” glass wafers. An oxygen plasma, which cleaned the glass surface of organic contaminates, resulted in extremely hydrophilic surfaces. Subsequent hydrogen plasma was shown to dramatically modify the surface resulting in a more hydrophobic state. However, the contact angle gradually decreased within a few hours to a hydrophilic state comparable to the as-cleaned condition.

A potential mechanism to explain this behavior is hydrogen diffusion into the glass surface. Although hydrogen diffusion in glass at room temperature is very slow, the activated hydrogen ions in a plasma are likely trapped by the glass surface and diffuse at least a short distance. Removed from the PECVD chamber, the hydrogen is slowly released from the surface resulting in the eventual hydrophilic state. AFM measurements show no obvious difference in surface roughness after hydrogen plasma. This strongly suggests that the surface modification are not due to local restructuring of the glass surface.

References

- [1] Kenji Nomura, Hiromichi Ohta, Akihiro Takagi, Toshio Kamiya, Masahiro Hirano, and Hideo Hosono. "Room-temperature fabrication of transparent flexible thin-film transistors using amorphous oxide semiconductors." *Nature* 432, no. 7016 (2004): 488-492.
- [2] Kunigunde H. Cherenack, Niko S. Münzenrieder, and Gerhard Tröster. "Impact of mechanical bending on ZnO and IGZO thin-film transistors." *Electron Device Letters, IEEE* 31, no. 11 (2010): 1254-1256.
- [3] Jae Sang Lee, Seongpil Chang, Sang-Mo Koo, and Sang Yeol Lee. "High-performance a-IGZO TFT with gate dielectric fabricated at room temperature." *Electron Device Letters, IEEE* 31, no. 3 (2010): 225-227.
- [4] Chiao-Shun Chuang, Tze-Ching Fung, Barry G. Mullins, Kenji Nomura, Toshio Kamiya, Han-Ping David Shieh, Hideo Hosono, and Jerzy Kanicki. "P-13: Photosensitivity of Amorphous IGZO TFTs for Active-Matrix Flat-Panel Displays." In *SID Symposium Digest of Technical Papers*, vol. 39, no. 1, pp. 1215-1218. Blackwell Publishing Ltd, 2008.
- [5] Beom Soo Park, Dong Kil Yim, Seon-Mee Cho, Soo Young Choi, and John M. White. "(Invited) Novel Integration Process for IGZO MO-TFT Fabrication on Gen 8.5 PECVD and PVD Systems-A Quest to Improve TFT Stability and Mobility." *ECS Transactions* 54, no. 1 (2013): 97-102.
- [6] Hai Q. Chiang, Brian R. McFarlane, David Hong, Rick E. Presley, and John F. Wager. "Processing effects on the stability of amorphous indium gallium zinc oxide thin-film transistors." *Journal of Non-Crystalline Solids* 354, no. 19 (2008): 2826-2830.
- [7] Jae Kyeong Jeong, Jong Han Jeong, Hui Won Yang, Jin-Seong Park, Yeon-Gon Mo, and Hye Dong Kim. "High performance thin film transistors with cosputtered amorphous indium gallium zinc oxide channel." *Applied Physics Letters* 91, no. 11 (2007): 3505.
- [8] Hyeon-seok Bae, Jae-Hong Kwon, Seongpil Chang, Myung-Ho Chung, Tae-Yeon Oh, Jung-Ho Park, Sang Yeol Lee, James Jungho Pak, and Byeong-Kwon

- Ju. "The effect of annealing on amorphous indium gallium zinc oxide thin film transistors." *Thin Solid Films* 518, no. 22 (2010): 6325-6329.
- [9] Chen-Yang Chung, Bin Zhu, Dieter G. Ast, Raymond G. Greene, and Michael O. Thompson. "High mobility amorphous InGaZnO₄ thin film transistors formed by CO₂ laser spike annealing." *Applied Physics Letters* 106, no. 12 (2015): 123506.
- [10] Jin-Seong Park, H. Kim, and Il-Doo Kim. "Overview of electroceramic materials for oxide semiconductor thin film transistors." *Journal of Electroceramics* 32, no. 2-3 (2014): 117-140.
- [11] J. B. Kim, Canek Fuentes-Hernandez, William J. Potscavage Jr, X-H. Zhang, and Bernard Kippelen. "Low-voltage InGaZnO thin-film transistors with Al₂O₃ gate insulator grown by atomic layer deposition." *Applied Physics Letters* 94, no. 14 (2009): 142107.
- [12] Chih-Wei Chien, Cheng-Han Wu, Yu-Tang Tsai, Yen-Cheng Kung, Chang-Yu Lin, Po-Ching Hsu, Hsing-Hung Hsieh et al. "High-performance flexible a-IGZO TFTs adopting stacked electrodes and transparent polyimide-based nanocomposite substrates." *Electron Devices, IEEE Transactions on* 58, no. 5 (2011): 1440-1446.
- [13] Young-Bae Park, and Shi-Woo Rhee. "Effect of hydrogen plasma precleaning on the removal of interfacial amorphous layer in the chemical vapor deposition of microcrystalline silicon films on silicon oxide surface." *Applied Physics Letters* 68, no. 16 (1996): 2219-2221.
- [14] Narottam P. Bansal, and Robert H. Doremus. *Handbook of glass properties*. Elsevier, 2013.
- [15] John B Brady. "Diffusion data for silicate minerals, glasses, and liquids." *Mineral physics & crystallography: A handbook of physical constants* (1995): 269-290.
- [16] Masayuki Nogami, Kazuhiro Watanabe, Yuta Ito, Hiromasa Ito, and Hiromi Nakano. "Hydrogen Gas Reaction with Eu³⁺-Doped Al₂O₃-SiO₂ Glasses." *Journal of the American Ceramic Society* 93, no. 6 (2010): 1663-1667.

- [17] Peter L. Bocko, and Gary R. Trott. "Glass for the future: Displays and semiconductors." In *VLSI Circuits (VLSIC), 2013 Symposium on*, pp. C86-C89. IEEE, 2013.
- [18] Ying Wang, Weijin Chen, Biao Wang, and Yue Zheng. "Ultrathin Ferroelectric Films: Growth, Characterization, Physics and Applications." *Materials* 7, no. 9 (2014): 6377-6485.
- [19] ABRAHAM MARMUR, and MICHAEL D. LELAH. "The spreading of aqueous surfactant solutions on glass." *Chemical Engineering Communications* 13, no. 1-3 (1981): 133-143.
- [20] Thomas Young. "An essay on the cohesion of fluids." *Philosophical Transactions of the Royal Society of London* (1805): 65-87.
- [21] Haldor Topsoe. "Geometric factors in four point resistivity measurement." *Bulletin* 472-13 (1968): 63.
- [22] K. Vanheusden, C. H. Seager, WL T. Warren, D. R. Tallant, and J. A. Voigt. "Correlation between photoluminescence and oxygen vacancies in ZnO phosphors." *Applied Physics Letters* 68, no. 3 (1996): 403-405.
- [23] Nathaniel Walsh. "Passivation of Amorphous Indium-Gallium-Zinc Oxide (IGZO) Thin-Film Transistors." (2014).
- [24] Leo A. Wall, and Roland E. Florin. "Effect of Structure on the Thermal Decomposition of Polymers." *Journal of Research of the National Bureau of Standards* 60, no. 5 (1958): 451.
- [25] A. U. Alam, M. M. R. Howlader, and M. J. Deen. "The effects of oxygen plasma and humidity on surface roughness, water contact angle and hardness of silicon, silicon dioxide and glass." *Journal of Micromechanics and Microengineering* 24, no. 3 (2014): 035010.